

# We are IntechOpen, the world's leading publisher of Open Access books Built by scientists, for scientists

6,900

Open access books available

186,000

International authors and editors

200M

Downloads

Our authors are among the

154

Countries delivered to

TOP 1%

most cited scientists

12.2%

Contributors from top 500 universities



WEB OF SCIENCE™

Selection of our books indexed in the Book Citation Index  
in Web of Science™ Core Collection (BKCI)

Interested in publishing with us?  
Contact [book.department@intechopen.com](mailto:book.department@intechopen.com)

Numbers displayed above are based on latest data collected.  
For more information visit [www.intechopen.com](http://www.intechopen.com)



---

# Anticorrosive, Antimicrobial, and Bioactive Titanium Dioxide Coating for Surface-modified Purpose on Biomedical Material

---

Hsi-Kai Tsou and Ping-Yen Hsieh

Additional information is available at the end of the chapter

<http://dx.doi.org/10.5772/intechopen.68854>

---

## Abstract

A multifunctional titanium dioxide (TiO<sub>2</sub>) coating was used to provide anticorrosive, antimicrobial, and bioactive properties for the surface modification of biomedical materials because TiO<sub>2</sub> has a stable bonding structure, photocatalytic characteristics, and negatively charged surfaces in nature. For successful deposition, an arc ion plating technique was adopted to deposit the TiO<sub>2</sub> coating. The antimicrobial activity values of anatase-TiO<sub>2</sub>-coated stainless steel specimens against *Staphylococcus aureus* and *Escherichia coli* were 3.0 and 2.5, respectively, which are far beyond the value designated in JIS Z2801:2000 industrial standard. TiO<sub>2</sub> coatings on stainless steel also generate an increased (i.e., less negative) corrosion potential and decreased corrosion current in a sodium chloride solution, showing a reduced tendency and rate of substrate dissolution as well as a reduced coating of species into the electrolyte. In addition, TiO<sub>2</sub> coatings, especially with rutile phase, satisfied the requirements for activating the biological property of a polymeric polyetheretherketone surface. Therefore, TiO<sub>2</sub> is a promising surface modification for the biomedical materials used in surgical instruments and implants.

**Keywords:** anticorrosive, antimicrobial, bioactive, titanium dioxide, biomedical material

---

## 1. Introduction

Biomedical material is any substance that has been engineered to interact with biological systems for a medical purpose, which may be therapeutic (i.e., to treat, augment, repair, or replace malfunctioning tissue in the body) or diagnostic. Among the various types of biomedical materials, metallic materials are the most widely used because of their high load-supporting capacity, desirable qualities of wear and friction, and acceptable biocompatibility. Stainless

steel, titanium, and their alloys are considered especially promising materials for surgical instruments and implants of many types and sizes. Polymeric materials have also garnered considerable interest in research and development as soft- and hard-tissue replacements, on the basis of the ease of manufacturing and modifying such materials, and their appropriate physical, chemical, and mechanical properties.

When biomedical materials come in contact with physiological tissue and body fluids, various interactions, such as corrosive reaction, inflammation, and host response, are triggered. For this reason, knowing and understanding the surface properties of biomedical materials are crucial. Unfortunately, metallic materials are easily influenced by corrosion damage due to electrochemical reactions; additionally, the bioinertness and hydrophobic surface properties render polymeric materials unfavorable for cell adhesion. Long-term clinical experiments have also indicated that the primary causes of implant failure include not only unstable implant fixation to bone tissue, but also bacterial infection.

To overcome the aforementioned problems, a surface modification technique that uses a multifunctional titanium dioxide ( $\text{TiO}_2$ ) coating is introduced to provide anticorrosive, antimicrobial, and bioactive properties for the underlying biomaterial. These versatile natural features of  $\text{TiO}_2$  are attributed to its stable bonding structure, photocatalytic characteristics, and negatively charged surfaces. In this paper, a brief overview of  $\text{TiO}_2$  coating modification in the field of biomedical material is provided. The two main topics discussed in the next section are as follows:

- Antimicrobial and anticorrosive titanium dioxide coating on stainless steel to reduce hospital-acquired infection.
- Bioactive titanium dioxide coating on polyetheretherketone for spinal implant application.

## **2. Antimicrobial and anticorrosive titanium dioxide coating on stainless steel to reduce hospital-acquired infection**

### **2.1. Background**

The increasing incidence and host risk of device-related infections that result in morbidity and even mortality have been noted for some time, particularly regarding the spread of antibiotic-resistant bacteria, such as methicillin-resistant *Staphylococcus aureus* and bursting *Clostridium difficile*. These hospital-acquired infections are a worldwide problem [1]. The outbreaks of SARS and avian influenza have also drawn attention to novel preventative measures, including the development and application of antimicrobial materials, to enhance the conventional disinfection concept. This movement compelled us to develop an antimicrobial technique for medical implements in clinical use.

Antimicrobial or antibacterial refers to the inhibition of bacterial growth and reproduction [2]. Antimicrobial functions can be performed by essential materials themselves or through the use of coating materials. One example of an essential antimicrobial alloy material is stainless steel that has been doped with copper. This material forms when  $\epsilon$ -copper precipitates in a

steel matrix; specifically, copper ions can be dissolved into a surface-passivated chromium oxide film. Such creates an antimicrobial effect on the stainless steel surface, resulting in the inhibition of bacterial growth [3]. The similar antimicrobial metal alloys, such as copper-containing ferritic stainless steel [4], martensitic stainless steel [5], and austenitic stainless steel [6], were also developed. On the other hand, for the antimicrobial purpose on coating materials, the idea of coatings containing with copper, silver, zinc, and other antimicrobial active metals was considered [7]. Unfortunately, such substance may induce the corrosion reaction because of the undesired Galvanic effect between two metals, which may be unsustainable during service. In this regard,  $\text{TiO}_2$  with anatase (A- $\text{TiO}_2$ ) phase may be the promising candidates for antimicrobial purposes.

The antimicrobial effects of  $\text{TiO}_2$  are attributed to its photocatalytic characteristics, as discovered by Fujishima and Honda [8]. The photocatalytic process of  $\text{TiO}_2$  involves the generation of electron-hole pairs when the material is exposed to light that emits energy exceeding the band gap energy of  $\text{TiO}_2$ . The aggressive superoxide ions ( $\text{O}^{2-}$ ) are generated by the electron attack, and the holes accelerate hydroxyl radical ( $\cdot\text{OH}$ ) formation on the material surface [9, 10]. These active radicals subsequently inhibit the growth of germs and bacteria that are known to be antimicrobially active through the direct oxidation of intracellular coenzyme, reducing the respiratory activity and thereby causing cell death [11].

In the present study, arc ion plating (AIP) was used to deposit a  $\text{TiO}_2$  coating on common medical-grade AISI 304 stainless steel. The antimicrobial efficacy of the  $\text{TiO}_2$ -coated stainless steel specimens was then evaluated according to the JIS standard. The corrosion resistance of the  $\text{TiO}_2$  coating was also examined to determine whether such films can be stable in a physiological environment. The results suggest that this modification may be effective as an antimicrobial surface coating for medical implements to reduce the risk of hospital-acquired infections.

## 2.2. Preparation of antimicrobial and anticorrosive $\text{TiO}_2$ films

$\text{TiO}_2$  deposition was conducted using a typical AIP technique and involved three steps: argon ion bombardment, bottom titanium layer deposition, and  $\text{TiO}_2$  coating deposition. The ion bombardment was performed to clean and mildly preheat the substrate, followed by the bottom titanium layer deposition, which enhanced the adhesion between the substrate and  $\text{TiO}_2$  coating.

The wide acceptance indicates that an A- $\text{TiO}_2$  phase structure is the key factor for maximizing the antimicrobial efficiency of  $\text{TiO}_2$ . This corresponds to a specific condition with 100% oxygen pressure at 0.5 Pa by using the AIP technique with a cathode target voltage of 20 V and a cathode target current of 90 A. Under this optimized deposition condition, the proportion of A- $\text{TiO}_2$  in the  $\text{TiO}_2$  coating has been reported to be 76.8% [12–14].

## 2.3. Antimicrobial characteristics of $\text{TiO}_2$ -coated stainless steel

The JIS Z2801:2000 [15] was employed as a standard to test the antimicrobial efficacy of  $\text{TiO}_2$ -coated stainless steel specimens. The bacterial strains used in this test were Gram-positive *Staphylococcus aureus* (*S. aureus*, ATCC 6538P) and Gram-positive *Escherichia coli* (*E. coli*, ATCC 8739) with an initial concentration of  $4.0 \times 10^5$  bacteria/mL. In the antimicrobial test,

the specimens were divided into three groups: group A and group B consisted of uncoated stainless steel specimens, and group C consisted of TiO<sub>2</sub>-coated stainless steel specimens. The specimens in group A immediately underwent serial dilution and plate culture after inoculation, while the specimens of groups B and C were incubated with exposure to fluorescent lighting for 24 h. The fluorescent lamp used was a regular daily-living light source that emitted mainly visible light and had a weak emission of 365 nm. Antimicrobial activity (*R*) of the specimens in all three groups was then calculated.

As revealed in **Figure 1** [13], the petri dishes corresponding to groups A and B (the uncoated stainless steel specimens) presented significant numbers of *S. aureus* and *E. coli* bacterial colonies, respectively; by contrast, the TiO<sub>2</sub>-coated stainless steel specimens in group C did not show a significant amount of bacterial colonies. This qualitatively describes the antimicrobial ability of the TiO<sub>2</sub> coating. Although only one out of the three petri dishes corresponding to each group is pictured in **Figure 1**, those not shown revealed a similar situation; this confirms the statistical accuracy of the antimicrobial test.

For both *S. aureus* and *E. coli*, the numbers of viable bacteria for groups A, B, and C are compared in **Figure 2** [13]. The group A specimens showed  $2.85 \times 10^5$  and  $1.06 \times 10^5$  viable bacteria cells, respectively, for *S. aureus* and *E. coli*, whereas the group B specimens showed  $1.04 \times 10^4$  and  $1.36 \times 10^4$  viable bacteria cells, respectively, for *S. aureus* and *E. coli*. By contrast, the group C specimens showed no bacterial colonies (10 bacteria cells) for *S. aureus* and  $4.30 \times 10^1$  viable bacteria cells for *E. coli*. Based on these results, the TiO<sub>2</sub>-coated stainless steel specimens presented *R* values of 3.0 and 2.5, respectively, for *S. aureus* and *E. coli*. Such values are far beyond the index of 2 stipulated for the JIS test standard.

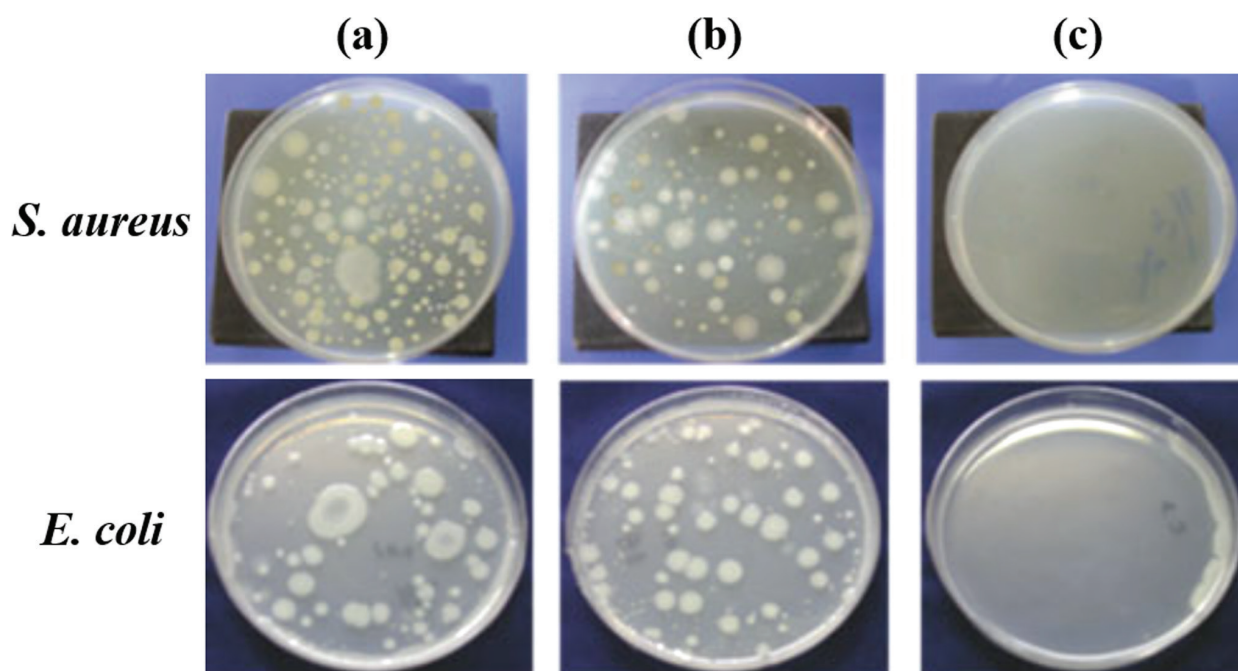


**Figure 1.** *S. aureus* and *E. coli* colonies formed on petri dishes after 24 h on the (a) group A stainless steel specimens, (b) group B stainless steel specimens, and (c) TiO<sub>2</sub>-coated stainless steel specimens [13].

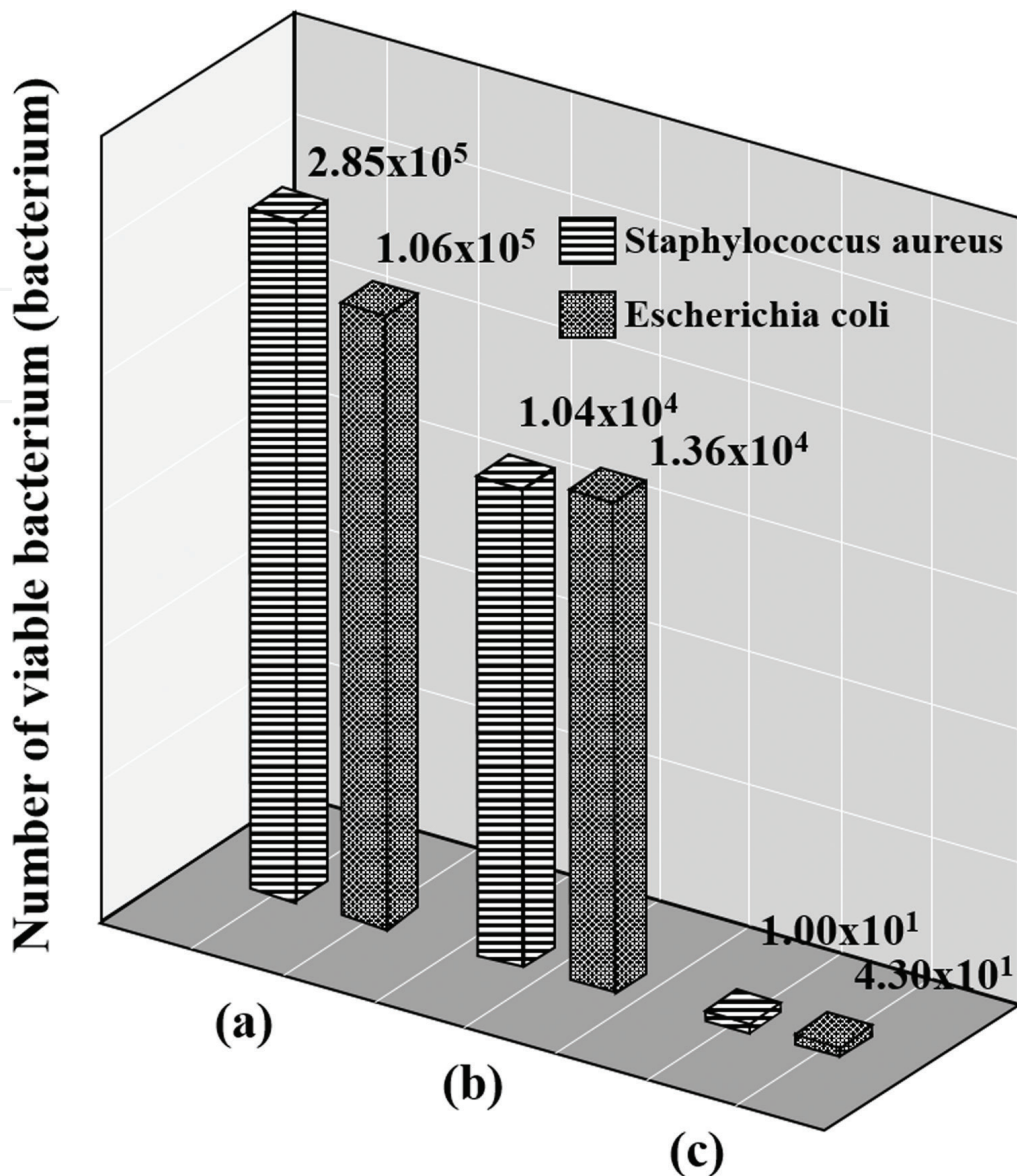


**Figure 2.** Viable bacteria numbers of *S. aureus* and *E. coli* for (a) group A stainless steel specimens, (b) group B stainless steel specimens, and (c) TiO<sub>2</sub>-coated stainless steel specimens [13].

To further investigate the antimicrobial mechanism of a TiO<sub>2</sub> coating, the bacterial microstructure was observed using transmission electron microscopy (TEM; JEOL JEM-1230). This closer examination revealed that most of the *S. aureus* cells were retained their integrity as the cells were inoculated on bare stainless steel with the exposure to fluorescent light for 24 h; moreover, the complete cell structure, including the cell wall, cytoplasmic membrane, cytoplasm, and nucleoid, was observed. The cells were undergoing mitosis, as presented in **Figure 3(a)** [14], was also found. These results indicate that the inoculated *S. aureus* cells on bare stainless steel were not deactivated by the fluorescent light. However, for the *S. aureus* cells on the TiO<sub>2</sub>-coated stainless steel specimens, detachment of the cell wall from the cell membrane was frequently observed in the microscopic field (**Figure 3(b)** [14]). As has been noted elsewhere [16–18], the cell walls in these specimens are attacked by superoxide ions and

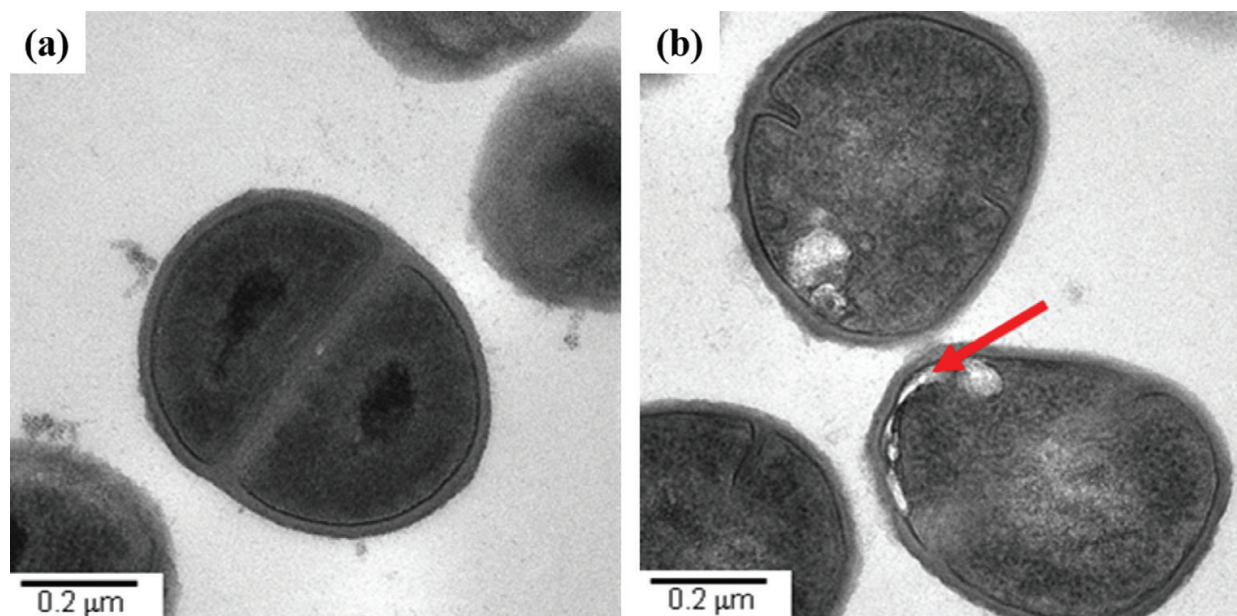


**Figure 3.** Cell structures of *S. aureus* inoculated on (a) bare stainless steel and (b)  $\text{TiO}_2$ -coated stainless steel specimens, following continuous exposure to a fluorescent lamp for 24 h. (The arrow indicates detachment of cell wall from the cell membrane.) [14].

hydroxyl radicals, and lipid peroxidation caused polyunsaturated phospholipids in the cell membrane to be destroyed; similarly, the degeneration of the membranes in the present study caused the detachment of the cell walls from the cell membranes.

A high percentage of the *E. coli* cells inoculated on bare stainless steel and exposed to fluorescent light for 24 h also retained their integrity, as depicted in **Figure 4(a)** [14]. By contrast, a large amount of *E. coli* cell fragments were observed following inoculation on  $\text{TiO}_2$ -coated stainless steel specimens and exposure to fluorescent light for 24 h, as presented in **Figure 4(b)** [14]. This occurred because *E. coli* cell walls are too thin to protect against attack by superoxide ions and hydroxyl radicals, resulting in massive death. A closer examination of the *E. coli* cells reveals that the nucleoid structures in the cytoplasm tend to give way to features of condensation, as indicated by the arrow in **Figure 4(b)**. The degeneration of *E. coli* in response to photocatalysis found in the present study is similar to the degeneration that was observed in response to the antimicrobial effects of silver ions [16].

#### 2.4. Anticorrosive characteristics of $\text{TiO}_2$ -coated stainless steel

A potentiodynamic polarization test was carried out in a potentiostat (EG&G 263 A) according to the ASTM G44–99 standard [19] to evaluate the corrosion resistance of a  $\text{TiO}_2$  coating in a 3.5 wt.% sodium chloride electrolyte. A saturated silver/silver chloride electrode was used as the reference, with a platinum counter electrode; a  $\text{TiO}_2$ -coated stainless steel specimen was inserted as the working electrode.

**Figure 5** illustrates the potentiodynamic polarization curves of bare stainless steel and  $\text{TiO}_2$ -coated stainless steel specimens [20]. The corrosive potential ( $E_{\text{corr}}$ ) and corrosive current ( $I_{\text{corr}}$ ) were  $-0.54$  V and  $6.0 \times 10^{-8}$  A/cm<sup>2</sup>, respectively, for the bare stainless steel

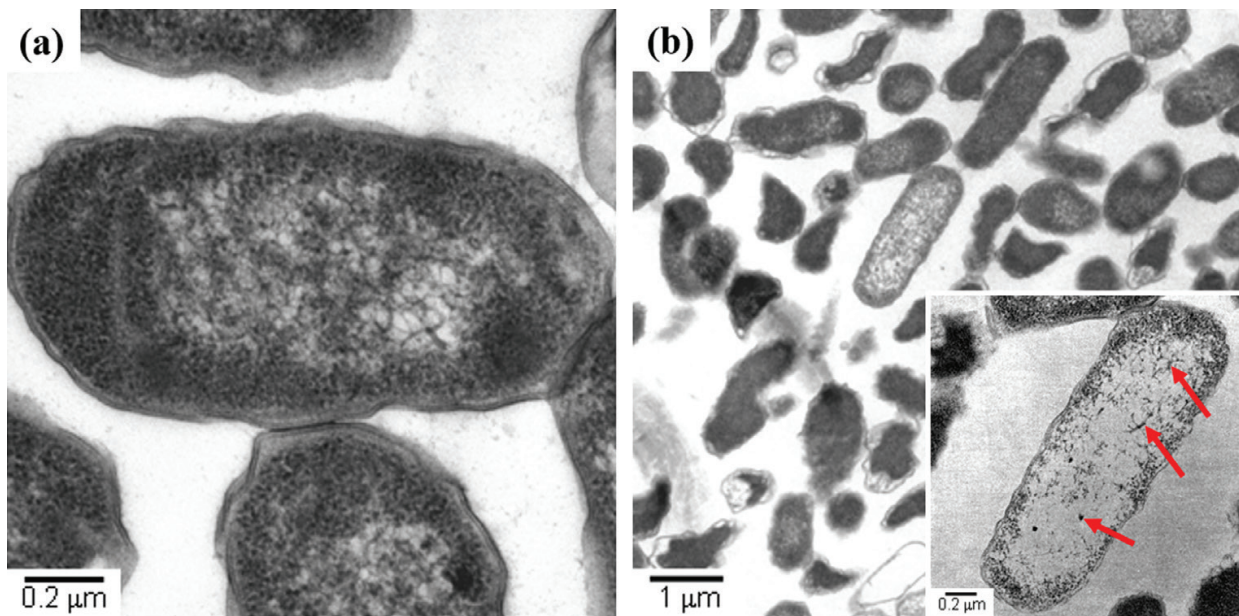


**Figure 4.** Cell structures of *E. coli* inoculated on (a) bare stainless steel and (b) TiO<sub>2</sub>-coated stainless steel specimens, following continuous exposure to a fluorescent lamp for 24 h. (The arrows indicate the condensation features of the nucleoid) [14].

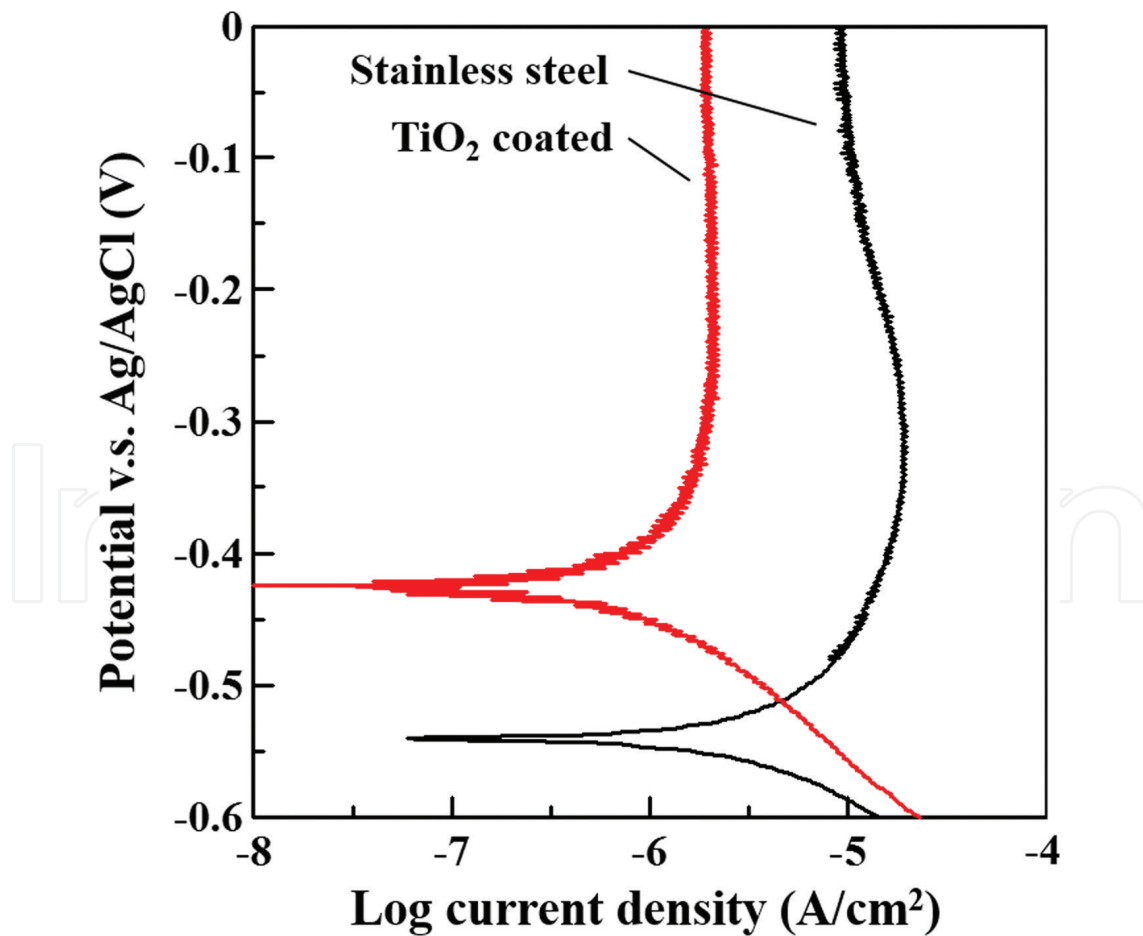


**Figure 5.** Polarization curves of bare stainless steel and TiO<sub>2</sub>-coated stainless steel specimens in a 3.5 wt.% sodium chloride solution [20].

specimens. Once the specimens had been coated with  $\text{TiO}_2$ , the  $E_{\text{corr}}$  and  $I_{\text{corr}}$  of the specimens were  $-0.42\text{ V}$  and  $1.0 \times 10^{-8}\text{ A/cm}^2$ , respectively. Notably,  $\text{TiO}_2$  is an inorganic compound, and its inertness in corrosive environments (e.g., a sodium chloride solution) helps reduce the tendency and rate of substrate dissolution and species coating in an electrolyte. This increases the corrosive potential and decreases the corrosive current, as noted herein.

In summary, the research results show that A- $\text{TiO}_2$  adds effective antimicrobial characteristics to stainless steel. The key to providing efficient antimicrobial efficacy lies in the photocatalytic performance of the coating, which originates from the anatase phase. Furthermore, based on the TEM observation results, the antimicrobial mechanisms that inhibit *S. aureus* and *E. coli* bacteria under the photocatalytic action of A- $\text{TiO}_2$  are different; specifically, the antimicrobial efficacy of A- $\text{TiO}_2$  against *E. coli* is more thorough. The A- $\text{TiO}_2$  coating also reduces the overall rate of corrosion and increases the corrosion barrier, compared with the features of bare stainless steel.

### 3. Bioactive titanium dioxide coating on polyetheretherketone for spinal implant application

#### 3.1. Background

Orthopedic implants have become one of the most highly developed fields in hard-tissue replacement. Polyetheretherketone (PEEK) polymer, with its high chemical resistance, radiolucency to X-ray scanning, and low elastic modulus similar to human cancellous bone, has become a highly preferred biomaterial, providing a promising alternative to metallic implants [21]. In particular, the elastic modulus can avoid the stress shielding effect, and prevent compression fractures and osteopenia syndrome; the X-ray radiolucency characteristic does not present a medical image shielding problem. PEEK can also be sterilized and shaped by machining to fit the contour of bones [22]. Consequently, PEEK has been widely used for load-bearing orthopedic applications, including dental implants, screws, and spinal interbody fusion cages [23, 24].

Despite these excellent properties, PEEK is still categorized as a bioinert material because of its hydrophobic feature and inertness with the surrounding tissue [21]. To overcome this problem, two primary strategies, bulk modification and surface modification, have been proposed to enhance the bone fusion ability of the PEEK. Bulk modification incorporates various bioactive materials, such as hydroxyapatite (HA) [25], strontium-containing hydroxyapatite [26],  $\beta$ -tricalcium phosphate [27], or  $\text{TiO}_2$  [28], into the PEEK matrix to form PEEK-based biocomposites. However, their tensile strength and toughness decrease as more of the bioactive materials are added, resulting in a substantial increase in the elastic modulus of these biomedical composites; the biomechanical property of these PEEK-based biocomposites is therefore no longer similar to that of human cancellous bone [21]. Conversely, surface modification only alters the surface properties of a material, without adversely affecting its bulk properties. In other words, surface modification is a more suitable approach for adapting PEEK to be used as implant. Consequently, various surface modification approaches have been developed to promote the

hydrophilic and biological characteristics of PEEK, such as using plasma treatment to change the surface chemistry [29], using chemical treatment to graft functional groups [30], and using laser treatment to roughen the surface [31]. Moreover, adding a functional coating to PEEK to create a bioactive surface is a more effective method for enhancing osseointegration performance [32–38]. Functional coating materials include HA [32], titanium [33, 34], TiO<sub>2</sub> [35–37], and diamond-like carbon [38]. To date, by taking the advantage of good biocompatibility of titanium with human body, very thick titanium produced over PEEK surface via vacuum plasma spray for spinal implant has been clinically available.

It has been well established that under humid conditions, the surface of TiO<sub>2</sub> generates hydroxyl groups (–OH<sup>-</sup>), followed by the conjunction with calcium ions (Ca<sup>2+</sup>) and phosphate groups (PO<sub>4</sub><sup>3-</sup>) from physiological fluid. Therefore, bone-like apatite compounds can be formed on the TiO<sub>2</sub> surface to induce osteoblast cell adhesion and proliferation [39, 40]. Based on the results, TiO<sub>2</sub> has been reported to exhibit excellent biocompatibility and further classified as a bioactive material [39, 40]. Furthermore, TiO<sub>2</sub> demonstrated excellent osseointegration ability, according to the animal experiment study [41]. These biological characteristics render TiO<sub>2</sub> film an even more promising material for the successful modification of PEEK surfaces, in comparison with regular titanium film.

In this research, the AIP technique was used to deposit TiO<sub>2</sub> films with controllable A-TiO<sub>2</sub> and rutile (R-TiO<sub>2</sub>) phases onto PEEK substrates. The investigation focused on determining the effects of introducing a TiO<sub>2</sub> coating on the *in vitro* and *in vivo* characteristics of TiO<sub>2</sub>-coated PEEK specimens, and evaluating the ability of the modified PEEK in a clinical application to shorten the osseointegration period for spinal implants and bone tissues.

### 3.2. Preparation of biocompatible TiO<sub>2</sub> films

The detailed AIP-TiO<sub>2</sub> deposition work is described in Section 2.2. The deposition conditions used in this section are listed in **Table 1**; target current and substrate bias were systematically manipulated to achieve specific ratios of A-TiO<sub>2</sub> and R-TiO<sub>2</sub> in the deposited films, characterized by a fixed 100% oxygen pressure of 0.5 Pa and a cathode target voltage of 20 V.

Based on the microstructure characteristics results [12], the AIP process can successfully fabricate TiO<sub>2</sub> films of varying A-TiO<sub>2</sub> and R-TiO<sub>2</sub> composition when appropriate coating parameters are used. Specifically, the A-TiO<sub>2</sub> phase in the deposited films ranged from 9.1% to 92.7% (**Table 1**).

Sample code	Target current (A)	Substrate bias (V)	A-TiO <sub>2</sub> content (%)
60A0V	60	0	92.7
90A0V	90	0	76.8
90A20V	90	-20	46.6
90A25V	90	-25	21.5
90A30V	90	-30	9.1

**Table 1.** Deposition conditions and the proportions of A-TiO<sub>2</sub> phases for TiO<sub>2</sub> coatings.

A low target current promotes the growth of A-TiO<sub>2</sub>, whereas a high substrate bias induces the formation of R-TiO<sub>2</sub>. The mechanism behind this outcome was previously investigated [12].

### 3.3. *In vitro* characteristics of TiO<sub>2</sub>-coated PEEK

First, the MC3T3-E1 osteoblast cell line was used in the osteoblast compatibility test to assess the cell adhesion test, cell proliferation test, cell differentiation test, and osteogenesis performance [namely quantification of osteopontin (OPN), osteocalcin (OCN), and calcium content]. Next, the cell morphology that had attached to the PEEK and TiO<sub>2</sub>-coated PEEK specimens was observed using field emission scanning electron microscopy (FESEM; Hitachi S-4800).

**Figure 6** shows the osteoblast cell adhesion ability, cell proliferation ability, cell differentiation ability, and osteogenesis performance on the PEEK and TiO<sub>2</sub>-coated PEEK specimens at various deposition conditions [36]. Notably, the osteoblast cell adhesion, proliferation, and differentiation abilities on TiO<sub>2</sub>-coated PEEK specimens were superior to the bare PEEK specimens for all of the deposition conditions. This indicates that all of the obtained TiO<sub>2</sub> coatings possessed cell induction capabilities, which led to accelerated cell adhesion and growth and increased cell proliferation and maturity. These three indicators confirmed the osteoblast compatibility of the TiO<sub>2</sub>-coatings deposited on PEEK. Furthermore, the osteogenesis performance (revealed by OPN, OCN, and calcium content as shown in **Figure 6(d)–(f)** [36], respectively) demonstrated that TiO<sub>2</sub> coatings also significantly increased the osteogenesis performance. This suggests that TiO<sub>2</sub> coatings enhance extracellular bone matrix growth. **Figure 6** [36] also shows that the specimen 90A30V, which was the richest in R-TiO<sub>2</sub> phase, exhibited the most osteoblast compatibility.

**Figure 7** shows the morphologies of the osteoblast cells after they were cultured for 0.5 and 48 h on PEEK and TiO<sub>2</sub>-coated PEEK specimens at different deposition conditions [36].

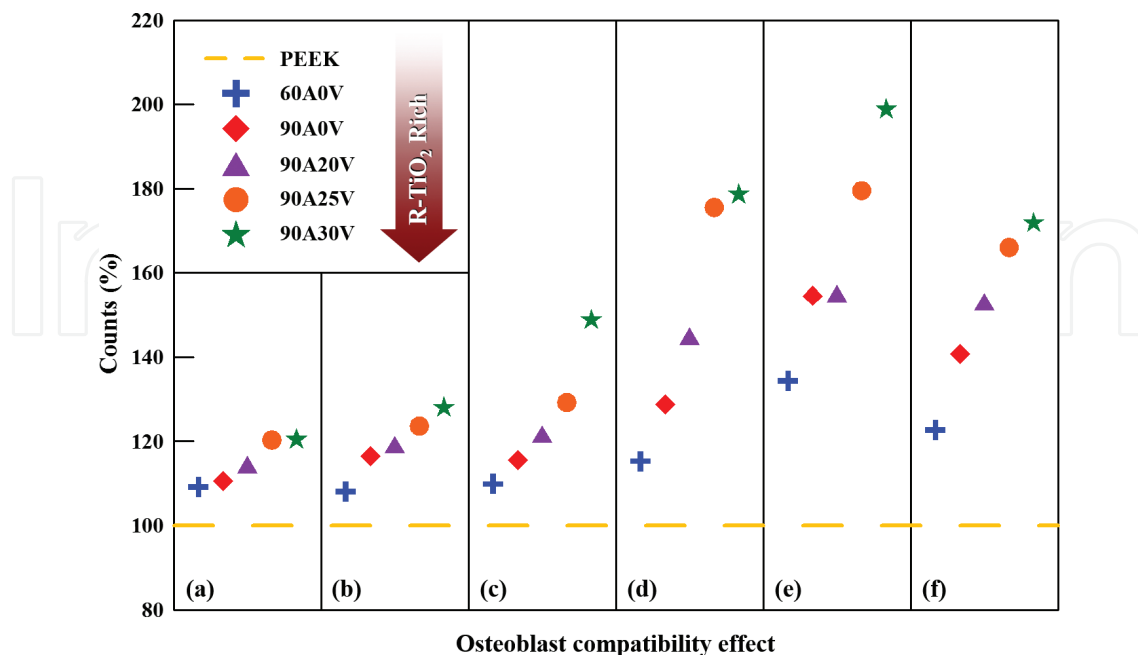


**Figure 6.** (a) Cell adhesion ability, (b) cell proliferation ability, (c) cell differentiation ability, (d) OPN, (e) OCN, and (f) calcium content of the osteoblast inoculated on bare PEEK and TiO<sub>2</sub>-coated PEEK specimens with various deposition conditions [36].

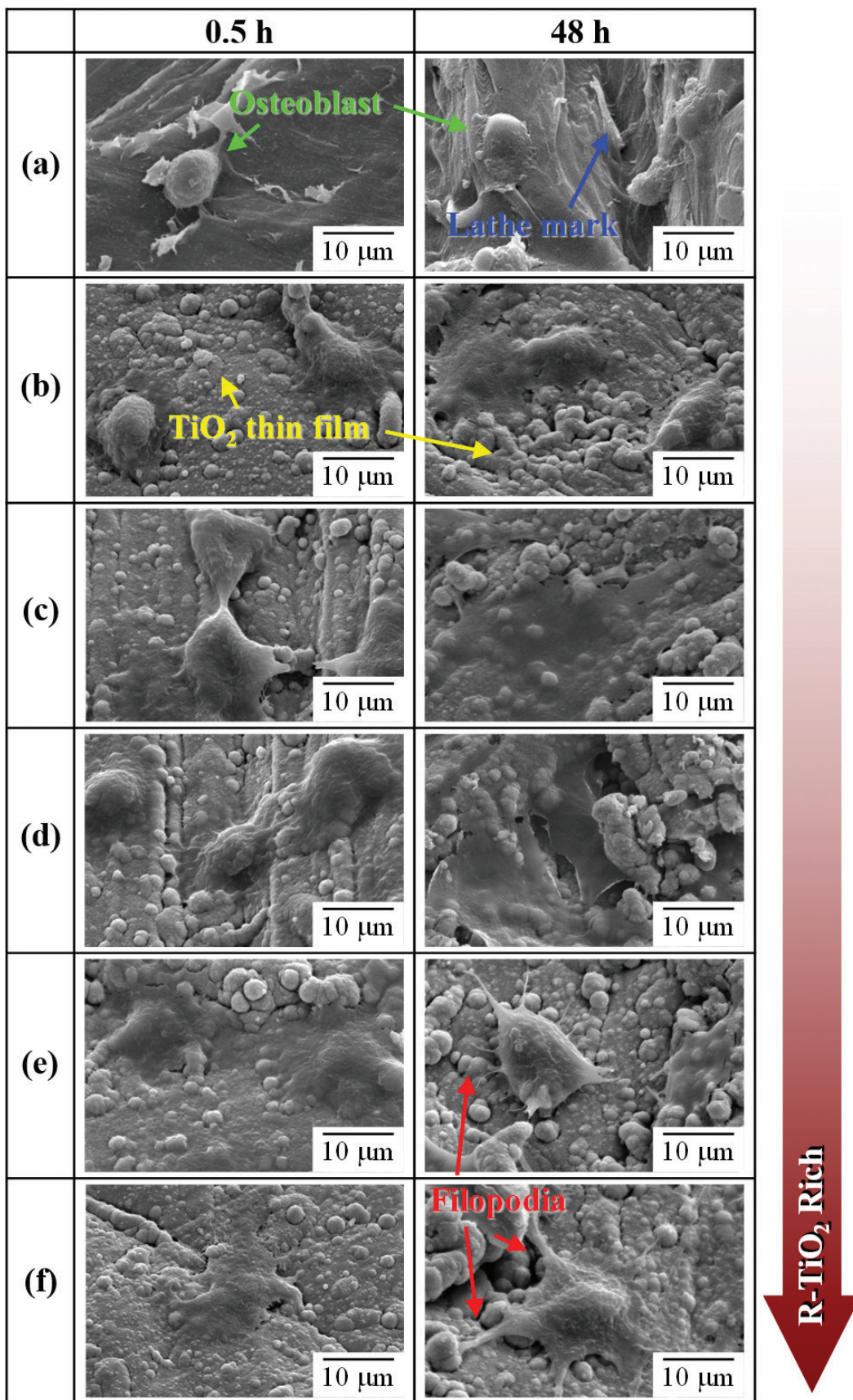


**Figure 7.** Morphologies of the osteoblasts cultured for 0.5 and 48 h on (a) the bare PEEK specimens, and the TiO<sub>2</sub>-coated PEEK specimens at different deposition conditions: (b) 60A0V, (c) 90A0V, (d) 90A20V, (e) 90A25V, and (f) 90A30V [36].

Specifically, the morphology of osteoblast cells on the bare PEEK specimens remained spherical without the appearance of filopodium, suggesting the poor adhesion to the specimen. By comparison, osteoblasts on the TiO<sub>2</sub>-coated PEEK specimens with the culturing time of 0.5 h showed a very comfortable adhesion features, that is, the filopodia extension and well-developed lamellipodia on the cells; this was particularly notable on the films with high ratios of R-TiO<sub>2</sub> to A-TiO<sub>2</sub>. Similar results were observed in the cells cultured for 48 h. Overall, these results further confirm that a deposited film with high R-TiO<sub>2</sub> content has superior osteoblast growth.

Furthermore, bare PEEK, and TiO<sub>2</sub>-coated PEEK specimens were then immersed in a simulated body fluid (SBF) for 1, 3, 7, 14, and 28 days, to investigate the effect of TiO<sub>2</sub> coating on the ability to induce HA formation. The TiO<sub>2</sub> coatings that possessed A-TiO<sub>2</sub> and R-TiO<sub>2</sub> under the deposition conditions of 60A0V and 90A30V, respectively, were examined. This biomimetic immersion test is a valuable approach for evaluating bioactivity of a candidate bone implant material prior to an *in vivo* test [42].

**Figure 8** illustrates the X-ray diffraction (XRD) patterns of bare PEEK, A-TiO<sub>2</sub>-coated PEEK, and R-TiO<sub>2</sub>-coated PEEK specimens after immersion in the SBF for a varying number of days [43]. During the early immersion period, the diffraction peaks that are ascribed to PEEK showed no observable change, indicating that the growing layer was undetectable in all of the specimens. After 28 days of immersion, weak and broadened diffraction peaks that are ascribed to HA were found, as shown in **Figure 8(a)** [43]. This implies that a very poor crystalline or even amorphous calcium phosphate layer had formed on the PEEK specimens. By contrast, after only 7 days and 3 days of immersion in the SBF solution, diffraction peaks that are ascribed to HA could be observed in A-TiO<sub>2</sub>- and R-TiO<sub>2</sub>-coated PEEK specimens, respectively. Over time, the intensity of these diffraction peaks increased significantly, as shown in **Figure 8(b)** and **(c)** [43], suggesting that additional crystalline HA was formed on them.

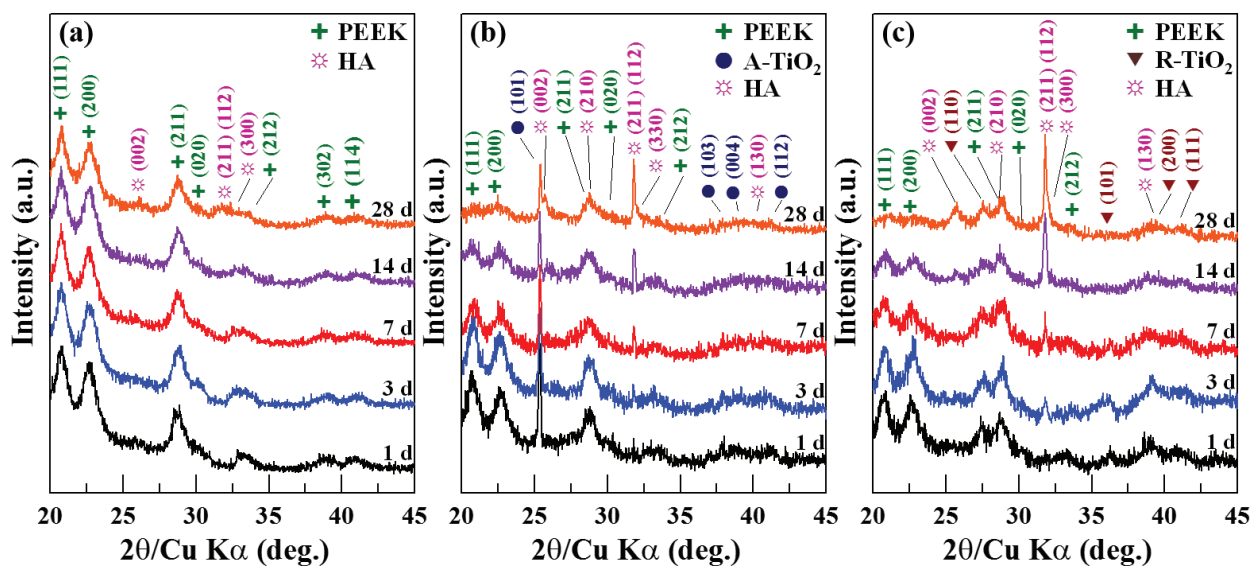


**Figure 8.** XRD patterns of the (a) bare PEEK, (b) A-TiO<sub>2</sub>-coated PEEK, and (c) R-TiO<sub>2</sub>-coated PEEK specimens immersed in a SBF for 1, 3, 7, 14, and 28 days [43].

Overall, these results suggest that HA growth in a SBF solution can be enhanced by adopting TiO<sub>2</sub> coatings, and that the R-TiO<sub>2</sub> coating seems to exhibit a superior capability to induce HA formation. Therefore, the results of the biomimetic immersion tests agree well with the finding of *in vitro* characteristics from osteoblast compatibility tests.

### 3.4. *In vivo* characteristics of TiO<sub>2</sub>-coated PEEK

Bullet-shaped PEEK implants with a diameter of  $\phi$  4.0 mm  $\times$  L 6.0 mm were used in an animal experiment. Bare PEEK, A-TiO<sub>2</sub>-coated PEEK, and R-TiO<sub>2</sub>-coated PEEK implants were inserted into the femurs of New Zealand white male rabbits to evaluate the *in vivo* osseointegration capacity through the push-out test and histological observation.

The push-out test can precisely quantify the degree of fixation between an implant and bone tissues [44]. **Figure 9** shows the push-out test results for the three implants after 4, 8, and 12 weeks [37]. Notably, the shear strength between the bone tissues and the implant increased as implantation time increased; at 12 weeks, the shear strength of the bare, A-TiO<sub>2</sub>-coated, and R-TiO<sub>2</sub>-coated PEEK implants was 2.54 MPa, 3.02 MPa, and 6.51 MPa, respectively. It was thus concluded that the bare PEEK implant had the poorest shear strength, but this could be enhanced by adding a TiO<sub>2</sub> coating. Overall, the R-TiO<sub>2</sub> coating had the optimal fixation.

To identify the failure mode between the implant and bone tissues after the push-out test, FESEM was adopted to observe the fracture morphology of the implant surface at 12 weeks, as shown in **Figure 10** [37]. It was noted that new bone tissue had fully peeled off the surface

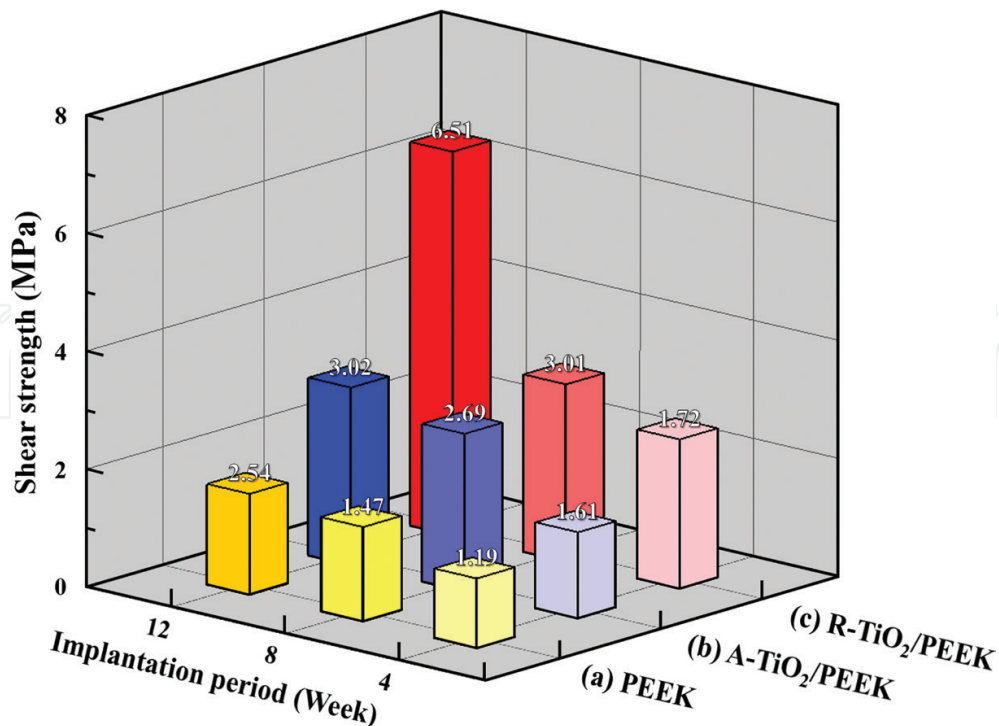


**Figure 9.** Shear strength between bone tissues and mplant for the (a) bare PEEK implant, (b) A-TiO<sub>2</sub>-coated PEEK implant, and (c) R-TiO<sub>2</sub>-coated PEEK implant at 4, 8, and 12 weeks after implantation [37].

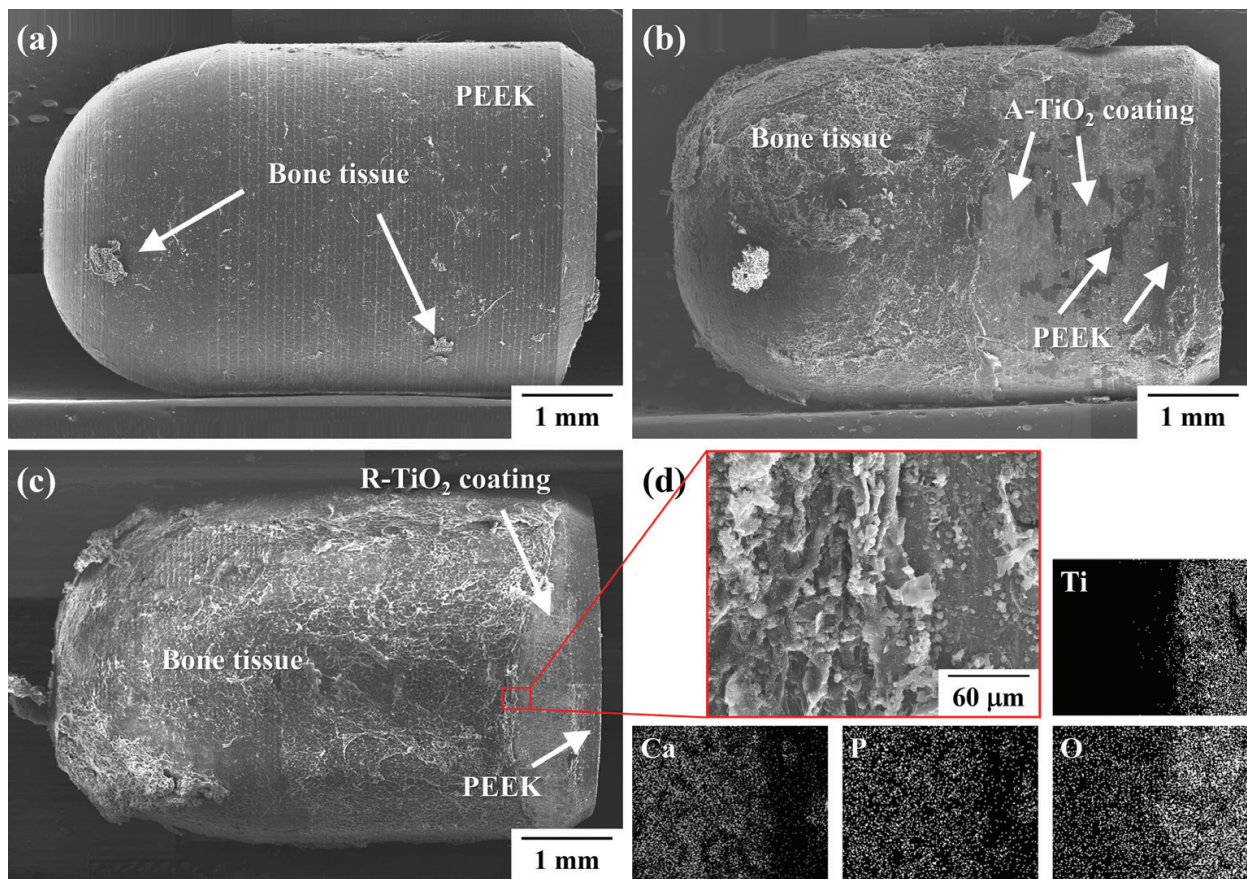


**Figure 10.** Fracture morphology of the (a) bare PEEK implant, (b) A-TiO<sub>2</sub>-coated PEEK implant, and (c) R-TiO<sub>2</sub>-coated PEEK implant with (d) the composition analysis of its bone tissues and implant interface after the push-out test conducted at 12 weeks [37].

of the bare PEEK implant (**Figure 10(a)** [37]), indicating that failure occurred at the bone/PEEK interface. Thus, the osseointegration capacity of a bare PEEK implant is poor. By contrast, when a TiO<sub>2</sub> coating was applied to the implant, a large area of the residual bone tissue adhered to the surface of the implant (**Figure 10(b)** and **(c)** [37]). Additionally, a particularly large amount of residual bone tissue on the R-TiO<sub>2</sub>-coated PEEK implant surface was confirmed by elemental mapping, as revealed in **Figure 10(d)** [37]. These analytical results indicate that TiO<sub>2</sub>-coated implants have a superior ability to induce bone growth and achieve bone ingrowth. The A-TiO<sub>2</sub>-coated PEEK implants experienced some coating detachment, resulting in a mixed adhesive failure between the A-TiO<sub>2</sub> coating and PEEK substrate, as well as cohesive failure of the bone itself. However, the R-TiO<sub>2</sub>-coated PEEK implant surfaces were almost completely covered with new bone tissue, almost no film detachment from the implants was observed, and thus, the failure can be regarded as cohesive failure by the bone tissue itself.

**Figure 11** depicts the histological sections of the three implants at 4, 8, and 12 weeks after implantation [37]. Notably, new bone tissue that was generated by bone remodeling had formed mature lamellar bone, and directly connected to the TiO<sub>2</sub>-coated PEEK implants after 4 weeks, indicating excellent osseointegration performance. Thus, it was concluded that

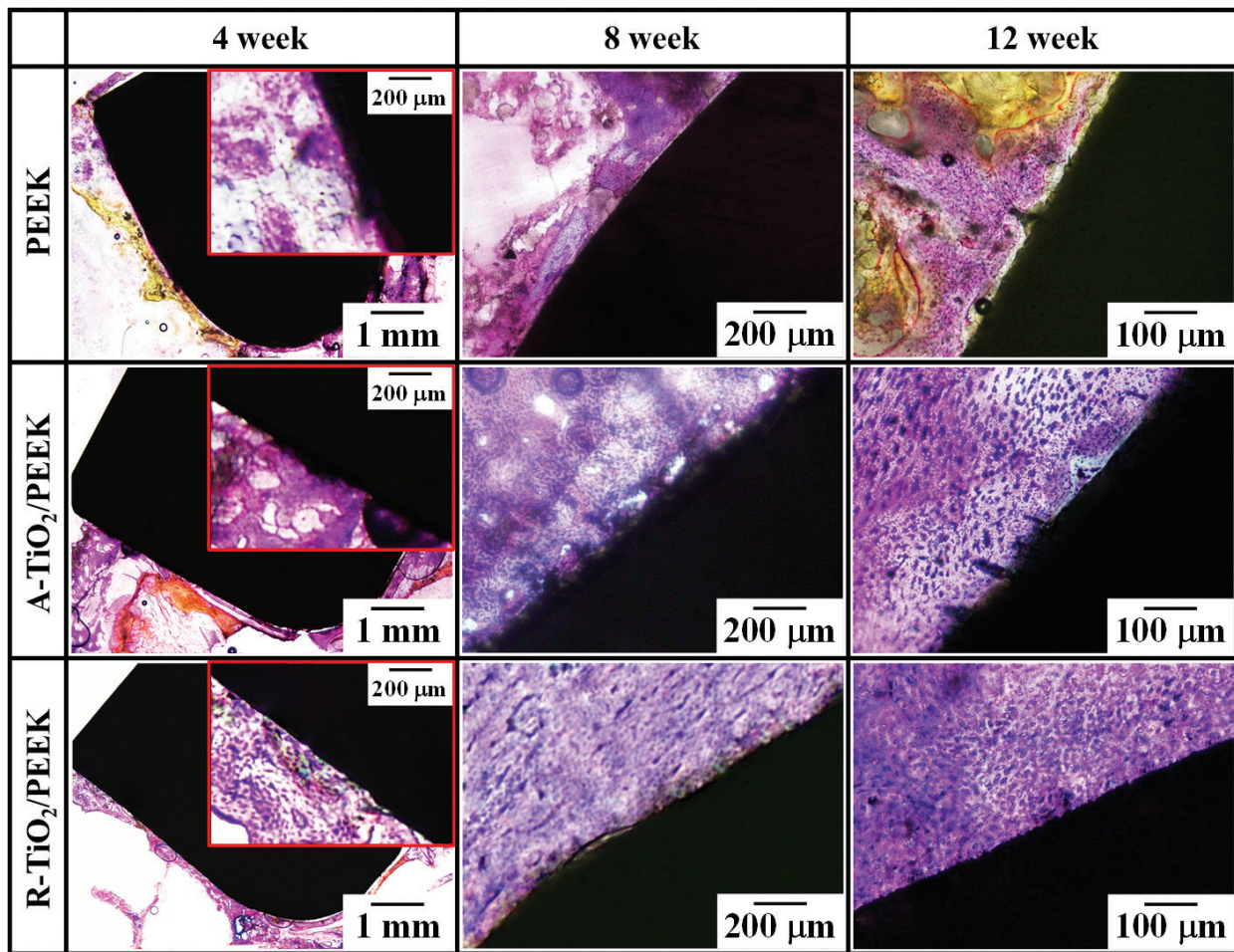


Figure 11. Histological sections of the bare PEEK implant, A-TiO<sub>2</sub>-coated PEEK implant, and R-TiO<sub>2</sub>-coated PEEK implant at 4, 8, and 12 weeks after implantation [37].

TiO<sub>2</sub> coating exhibits strong osteoblast compatibility and rapidly activates bone remodeling. Subsequently, the coating induced adhesion and proliferation of osteoblasts on the implant surface, and differentiation into osteocytes for the production of new bone tissue and later bone bonding. Conversely, new lamellar bone on the surface of the bare PEEK implants was not completely mature and not fully bonded with the implant.

The response of the TiO<sub>2</sub>-coated PEEK implants in the marrow cavity (located far from the cortical bone) at 4 weeks indicated that regenerated bone tissues grew onto the implant surfaces; moreover, this new bone is the result of bone tissue repair, which proliferates from the endosteum of cortical bone. Due to the osteoconductive effect, the new bone tissues grew inward to the implant surfaces in the marrow [45]. These findings indicate that TiO<sub>2</sub> coatings have excellent osteoconductivity and promote new bone growth on the TiO<sub>2</sub>-coated PEEK implant surfaces, with connections to cortical bone. By contrast, the surfaces of the bare PEEK implant were covered with fibrous tissue, implying that bone bonding did not occur between the implant and the cortical bone. Fibrous tissue growth is likely caused by micro movement in the implant and poor stability during the early implantation period [46].

When the implant period was extended to 8 weeks, immature osteogenesis was observed in the cortical bone around the bare PEEK implant, and new bone tissue was maturing after 12 weeks. However, fibrous tissue was still identified at the interface between the implants and bone tissues, indicating that the osseointegration capacity of bare PEEK implants is very limited, even when the implantation period is extended. By contrast, 8 weeks after the implantation of the TiO<sub>2</sub>-coated PEEK implants, histological sections in the marrow cavity revealed that the new bone tissue was maturing and osteocytes covered their surface. In other words, the osteoconductive effect of TiO<sub>2</sub> coating triggers quick bone remodeling. The new bone was fully mature and closely integrated with the TiO<sub>2</sub> coating in the cavity after 12 weeks (**Figure 11** [37]). However, a comparison of the TiO<sub>2</sub> coatings with different phase structures indicated that the degree of bone bonding between new bone and the R-TiO<sub>2</sub>-coated PEEK implant was significantly better than that between new bone and the A-TiO<sub>2</sub>-coated PEEK implant. In addition, some gaps existed between the A-TiO<sub>2</sub> coating and the new bone in some areas; detachment of the A-TiO<sub>2</sub> coating was also noted.

In summary, the *in vitro* and *in vivo* characteristics can be improved by TiO<sub>2</sub> coating because of its bioactivity; R-TiO<sub>2</sub> coatings perform particularly well, promoting biomimetic HA growth, osteoblast compatibility, and osseointegration. These phenomena are attributable to the abundance of negatively charged hydroxyl groups on the R-TiO<sub>2</sub> surface [35–37].

## 4. Conclusions

In this chapter, TiO<sub>2</sub> coatings prepared using the AIP technique to alter the surface properties of biomaterials were described. Specifically, it was found that introducing TiO<sub>2</sub> coating to stainless steel and PEEK specimens adds various anticorrosive, antimicrobial, and bioactive surface properties to the materials, which were systematically reviewed herein. The following conclusions can be drawn:

1. Owing to the efficient photocatalytic performance of its anatase phase structure, A-TiO<sub>2</sub>-coated stainless steel exhibits excellent antimicrobial efficacy against *S. aureus* and *E. coli* bacteria. The material could possibly serve as a new antimicrobial treatment for surgical instruments and medical implements to reduce the risk of hospital-acquired infections.
2. The high corrosion resistance of TiO<sub>2</sub> coatings in a 3.5 wt% sodium chloride solution was postulated as a direct consequence of its ceramic nature, suggesting that TiO<sub>2</sub> is electrochemically inert in the human body environment.
3. Based on the *in vitro* and *in vivo* tests, the bioactivity and osseointegration of all TiO<sub>2</sub> coatings were far superior to bioinert PEEK; moreover, R-TiO<sub>2</sub> coatings exhibited greater performance than A-TiO<sub>2</sub> coatings because of the abundance of negatively charged hydroxyl groups on its surface. Consequently, TiO<sub>2</sub>-coated PEEK specimens are suggested for use in clinical applications.
4. Overall, the aforementioned results prove that TiO<sub>2</sub> coatings are highly suitable for surface modifications of biomedical materials.

## Author details

Hsi-Kai Tsou<sup>1,2\*</sup> and Ping-Yen Hsieh<sup>3</sup>

\*Address all correspondence to: [tsouhsikai@gmail.com](mailto:tsouhsikai@gmail.com)

1 Functional Neurosurgery Division, Neurological Institute, Taichung Veterans General Hospital, Taichung City, Taiwan, ROC

2 Department of Rehabilitation, Jen-Teh Junior College of Medicine, Nursing and Management, Miaoli County, Taiwan, ROC

3 Department of Materials Science and Engineering, National Tsing Hua University, Hsinchu City, Taiwan, ROC

## References

- [1] Gottenbos B, Van der Mei HC, Klatter F, Grijpma DW, Feijen J, Nieuwenhuis P, Busscher HJ. Positively charged biomaterials exert antimicrobial effects on gram-negative bacilli in rats. *Biomaterials*. 2003;**24**:2707-2710
- [2] Kourai H. Surface science and microbiology: Antimicrobial finishings. *Journal of the Surface Science Society of Japan*. 2001;**22**:663-670
- [3] Morihiro H, Katsuhisa M, Sadao H, Michiyuki K, Seiichis I. Improving method of antibacterial performance of copper-containing stainless steel. *Japan Patent*. 1996;**08**:229107
- [4] Chungtsun TH, Tachiupao C, Kungnan KC. Antibacterial characteristic and material quality of ferrite antibacterial stainless steel "NSSAM-1". *Nisshin Steel Technical Report*. 1997;**76**:48-55
- [5] Chungtsun TH, Tachiupao CJ, Shanpen CJ. Corrosion quality of galvanized stainless steel. *Nisshin Steel Technical Report*. 1998;**77**:69-81
- [6] Shihyeh HH, Yutienchuan CK, Panching CN, Yuen KH. Antimicrobial pre-painted steel sheet. *Nisshin Steel Technical Report*. 1998;**78**:90-96
- [7] Kim TN, Feng QL, Kim JO, Wu J, Wang H, Chen GC, Cui FZ. Antimicrobial effects of metal ions (Ag<sup>+</sup>, Cu<sup>2+</sup>, Zn<sup>2+</sup>) in hydroxyapatite. *Journal of Materials Science: Materials in Medicine*. 1998;**9**:129-134.
- [8] Fujishima A, Honda K. Electrochemical photolysis of water at a semiconductor electrode. *Nature*. 1972;**238**:37-38
- [9] Cheng Q, Li C, Pavlinek V, Saha P, Wang H. Surface-modified antibacterial TiO<sub>2</sub>/Ag<sup>+</sup> nanoparticles: Preparation and properties. *Applied Surface Science*. 2006;**252**:4154-4160
- [10] Sawunyama P, Yasumori A, Okada K. The nature of multilayered TiO<sub>2</sub>-based photocatalytic films prepared by a sol-gel process. *Materials Research Bulletin*. 1998;**33**:795-801

- [11] Matsunaga T, Tomoda R, Nakajima T, Wake H. Photoelectrochemical sterilization of microbial cells by semiconductor powders. *FEMS Microbiology Letters*. 1985;**29**:211-214
- [12] Chung CJ, Tsou HK, Chen HL, Hsieh PY, He JL. Low temperature preparation of phase-tunable and antimicrobial titanium dioxide coating on biomedical polymer implants for reducing implant-related infections. *Surface and Coatings Technology*. 2011;**205**:5035-5039
- [13] Chung CJ, Lin HI, Tsou HK, Shi ZY, He JL. An antimicrobial TiO<sub>2</sub> coating for reducing hospital-acquired infection. *Journal of Biomedical Materials Research Part B: Applied Biomaterials*. 2008;**85B**:220-224
- [14] Chung CJ, Lin HI, Chou CM, Hsieh PY, Hsiao CH, Shi ZY, He JL. Inactivation of *Staphylococcus aureus* and *Escherichia coli* under various light sources on photocatalytic titanium dioxide thin film. *Surface and Coatings Technology*. 2009;**203**:1081-1085
- [15] JIS Z2801:2000. Antimicrobial products—Test for antimicrobial activity and efficacy. Japanese Industrial Standard. 2001
- [16] Huang Z, Maness PC, Blake DM, Wolfrum EJ, Smolinski SL. Bactericidal mode of titanium dioxide photocatalysis. *Journal of Photochemistry and Photobiology A: Chemistry*. 2000;**130**:163-171
- [17] Maness PC, Smolinski S, Blake DM, Huang Z, Wolfrum EJ, Jacoby WA. Bactericidal activity of photocatalytic TiO<sub>2</sub> reaction: Toward an understanding of its killing mechanism. *Applied and Environmental Microbiology*. 1999;**65**:4094-4098
- [18] Feng QL, Wu J, Chen GQ, Cui FZ, Kim TN, Kim JO. A mechanistic study of the antibacterial effect of silver ions on *Escherichia coli* and *Staphylococcus aureus*. *Journal of Biomedical Materials Research*. 2000;**52**:662-668
- [19] ASTM G44-99. Standard practice for exposure of metals and alloys by alternate immersion in neutral 3.5% sodium chloride solution. American Society for Testing and Materials. 2005
- [20] Chung CJ, Hsieh PY, Hsiao CH, Lin HI, Leyland A, Matthews A, He JL. Multifunctional arc ion plated TiO<sub>2</sub> photocatalytic coatings with improved wear and corrosion protection. *Surface and Coatings Technology*. 2009;**203**:1689-1693
- [21] Kurtz SM, Devine JN. PEEK biomaterials in trauma, orthopedic, and spinal implants. *Biomaterials*. 2007;**28**:4845-4869
- [22] Barton AJ, Sagers RD, Pitt WG. Bacterial adhesion to orthopedic implant polymers. *Journal of Biomedical Materials Research*. 1996;**30**:403-410
- [23] Williams DF, McNamara A, Turner RM. Potential of polyetheretherketone (PEEK) and carbon-fibre-reinforced PEEK in medical applications. *Journal of Materials Science Letters*. 1987;**6**:188-190.
- [24] Schwitalla A, Müller WD. PEEK dental implants: A review of the literature. *Journal of Oral Implantology*. 2013;**39**:743-749

- [25] Yu S, Hariram KP, Kumar R, Cheang P, Aik KK. In vitro apatite formation and its growth kinetics on hydroxyapatite/polyetheretherketon biocomposites. *Biomaterials*. 2005;**26**:2343-2352
- [26] Wong KL, Wong CT, Liu WC, Pan HB, Fong MK, Lam WM, Cheung WL, Tang WM, Chiu KY, Luk KDK, Lu WW. Mechanical properties and in vitro response of strontium-containing hydroxyapatite/polyetheretherketone composites. *Biomaterials*. 2009;**30**:3810-3817
- [27] Petrovic L, Pohle D, Münstedt H, Rechtenwald T, Schlegel KA, Rupprecht S. Effect of  $\beta$ TCP filled polyetheretherketone on osteoblast cell proliferation in vitro. *Journal of Biomedical Science*. 2006;**13**:41-46
- [28] Wu X, Liu X, Wei J, Ma J, Deng F, Wei S. Nano-TiO<sub>2</sub>/PEEK bioactive composite as a bone substitute material: In vitro and in vivo studies. *International Journal of Nanomedicine*. 2012;**7**:1215-1225
- [29] Ha SW, Kirch M, Birchler F, Eckert KL, Mayerv J, Wintermantel E, Sittig C, Pfund-Klingenfuss I, Textor M, Spencer ND, Guecheva M, Vonmont H. Surface activation of polyetheretherketone (PEEK) and formation of calcium phosphate coatings by precipitation. *Journal of Materials Science: Materials in Medicine*. 1997;**8**:683-690
- [30] Pino M, Stingelin N, Tanner KE. Nucleation and growth of apatite on NaOH-treated PEEK, HDPE and UHMWPE for artificial cornea materials. *Acta Biomaterialia*. 2008;**4**:1827-1836
- [31] Riveiroa A, Soto R, Comesaña R, Boutinguiza M, del Val J, Quintero F, Lusquiños F, Pou J. Laser surface modification of PEEK. *Applied Surface Science*. 2012;**258**:9437-9442
- [32] Wu GM, Hsiao WD, Kung SF. Investigation of hydroxyapatite coated polyether ether ketone composites by gas plasma sprays. *Surface and Coatings Technology*. 2009;**203**:2755-2758
- [33] Han CM, Lee EJ, Kim HE, Koh YH, Kim KN, Ha Y, Kuh SU. The electron beam deposition of titanium on polyetheretherketone (PEEK) and the resulting enhanced biological properties. *Biomaterials*. 2010;**31**:3465-3470
- [34] Walsh WR, Bertollo N, Christou C, Schaffner D, Mobbs RJ. Plasma-sprayed titanium coating to polyetheretherketone improves the bone-implant interface. *The Spine Journal*. 2015;**15**:1041-1049
- [35] Tsou HK, Hsieh PY, Chung CJ, Tang CH, Shyr TW, He JL. Low-temperature deposition of anatase TiO<sub>2</sub> on medical grade polyetheretherketone to assist osseous integration. *Surface and Coatings Technology*. 2009;**204**:1121-1125
- [36] Tsou HK, Hsieh PY, Chi MH, Chung CJ, He JL. Improved osteoblast compatibility of medical-grade polyetheretherketone using arc ion plated rutile/anatase titanium dioxide films for spinal implants. *Journal of Biomedical Materials Research Part A*. 2012;**100A**:2787-2792

- [37] Tsou HK, Chi MH, Hung YW, Chung CJ, He JL. In vivo osseointegration performance of titanium dioxide coating modified polyetheretherketone using arc ion plating for spinal implant application. *BioMed Research International*. 2015;**2015**:328943
- [38] Wang H, Xu M, Zhang W, Kwok DTK, Jiang J, Wu Z, Chu PK. Mechanical and biological characteristics of diamond-like carbon coated poly aryl-etherether-ketone. *Biomaterials*. 2010;**31**:8181-8187
- [39] Wu JM, Xiao F, Hayakawa S, Tsuru K, Takemoto S, Osaka A. Journal of Materials Science: Materials in Medicineacidic titanium tetrafluoride solution. *Journal of Materials Science: Materials in Medicine*. 2003;**14**:1027-1032
- [40] Lindberg F, Heinrichs J, Ericson F, Thomsen P, Engqvist H. Hydroxylapatite growth on single-crystal rutile substrates. *Biomaterials*. 2008;**29**:3317-3323
- [41] Erli HJ, Rüger M, Ragoß C, Jahnen-Dechent W, Hollander DA, Paar OO, von Walter M. The effect of surface modification of a porous TiO<sub>2</sub>/perlite composite on the ingrowth of bone tissue in vivo. *Biomaterials*. 2006;**27**:1270-1276
- [42] Kokubo T, Kim HM, Kawashita M. Novel bioactive materials with different mechanical properties. *Biomaterials*. 2003;**24**:2161-2175
- [43] Chi MH, Tsou HK, Chung CJ, He JL. Biomimetic hydroxyapatite grown on biomedical polymer coated with titanium dioxide interlayer to assist osteocompatible performance. *Thin Solid Film*. 2013;**549**:98-102
- [44] Dhert WJA, Jansen JA. The validity of a single pushout test. In: An YH, Draughn RA, editors. *Mechanical testing of bone and the bone-implant interface*. New York: CRC Press; 2000. pp. 477-487
- [45] Dua C, Meijer GJ, van de Valk C, Haan RE, Bezemer JM, Hesselning SC, Cui FZ, de Groot K, Layrolle P. Bone growth in biomimetic apatite coated porous Polyactive® 1000PEGT70PBT30 implants. *Biomaterials*. 2002;**23**:4649-4656
- [46] Søballe K, Hansen ES, Rasmussen HB, Jørgensen PH, Bünger C. Tissue ingrowth into titanium and hydroxyapatite-coated implants during stable and unstable mechanical conditions. *Journal of Orthopaedic Research*. 1992;**10**:285-299